Polímeros
ISSN 1678-5169 (Online)

https://doi.org/10.1590/0104-1428.20220024

ORIGINAL ARTICLE

Tuning the structure and properties of cell-embedded gelatin hydrogels for tumor organoids

Sarah Oliveira Lamas de Souza[1]*, Sérgio Mendes de Oliveira[1], Catarina Paschoalini Lehman[1], Mercês Coelho da Silva[2], Luciana Maria Silva[3] and Rodrigo Lambert Oréfice[1]

[1]Departamento de Engenharia Metalúrgica e de Materiais, Universidade Federal de Minas Gerais – UFMG, Belo Horizonte, MG, Brasil
[2]Universidade Federal de Itajubá – UNIFEI, Itabira, MG, Brasil
[3]Fundação Ezequiel Dias, Belo Horizonte, MG, Brasil
**sarahlamas@gmail.com*

Abstract

Tumor organoids have great potential as a 3D *in vitro* system to model cancer. In this work, we studied how the structure of hydrogels based on gelatin with methacryloyl groups (GeIMA) can affect their usage in tumor organoids. To this end, gelatin hydrogels with different levels of methacrylation and with cellulose nanocrystals (NCC) or reduced graphene oxide (rGO) were prepared and used to encapsulate human colon carcinoma cells (RKO). Mechanical properties of the hydrogels were measured in dynamic conditions at 37°C and water. Results showed that NCC was able to provide higher mechanical stability to the hydrogels. RKO cells embedded in GelMA were able to proliferate within the hydrogels, leading to the formation of groups of cells after 48 h. GelMA with higher crosslink densities and NCC tended to show higher cell population as possibly due to the higher level of stability and rigidity displayed by these hydrogels.

Keywords: *gelatin methacryloyl, GeIMA, hydrogels, organoid, three-dimensional cell culture.*

How to cite: Souza, S. O. L., Oliveira, S. M., Lehman, C. P., Silva, M. C., Silva, L. M., & Oréfice, R. L. (2023). Tuning the structure and properties of cell-embedded gelatin hydrogels for tumor organoids. *Polímeros: Ciência e Tecnologia*, *33*(2), e20230014. https://doi.org/10.1590/0104-1428.20220024

1. Introduction

In recent years, an in vitro 3D model alternative for human tissues, called organoids, has been increasingly studied. An organoid is a group of cells that has an organization similar to an organ or tissue, usually grown in a special 3D substrate[1,2]. Organoids can be used to model a disease, introducing mutations of the disease or using pluripotent cells derived from the patient to allow drug testing and tissue replacement therapies[3].

Cancerous organoids can be developed from patients with varying degrees and subtypes of cancer. Patient-derived organoids may have genetic backgrounds, while normal organoids can be used to model cancer evolution after the insertion of oncogenic mutations[3]. The behavior of cancer strains in tumor organoids can be monitored in real time by using microscopic images, as well as cell lines, which can be expanded and preserved to establish a live biobank[4].

Significant advances in biomaterials, especially hydrogels, have offered opportunities to facilitate the development of 3D systems that can be used in promising mini tumor organoids[5]. Biomacromolecule based-hydrogels can be designed to favor cell adhesion, proliferation, migration and differentiation, and provide cells with a highly hydrated 3D environment that mimics natural soft tissues[6]. Thus, the three-dimensional structure of hydrogels together with the encapsulation of cells has great potential as an alternative to tumor organoids as an effective cancer model to study the mechanisms of action and inhibition of tumor invasion[7].

Despite the remarkable achievements and technological progress of the last decade, developing a three-dimensional structure with efficient cellular application is still a difficult task[8]. Numerous approaches have been developed and tested in which they often presented non-scalable strategies and sometimes 3D conditions more similar to 2D cell culture.

Thus, in this work, the objective was to pursue the development of tumor organoids based on a three-dimensional matrix of gelatin methacryloyl (GeIMA). The structure and properties of GelMA were tuned by varying the crosslinking density, and by the incorporation of nanocomponents, such as cellulose nanocrystal (NCC) and reduced graphene oxide (rGO) to check the ability of this artificial extracellular matrix to support the growth of embedded human colon carcinoma cell lines (RKO AS45-1).

2. Materials and Methods

2.1 Materials

Gelatin from Porcine Skin Type A 300 Bloom (Sigma-Aldrich, G1890), Methacrylic Anhydride (MAA, Sigma-Aldrich, 276685), Dialysis Membrane Spectro /

MWCO 12-14 kDa (Fisher Scientific), 2-Hydroxy-4′-(2-hydroxyethoxy)-2-methylpropiophenone (Sigma-Aldrich, 410896-10G), Dulbecco's Modified Eagles Medium (DMEM), High Glucose (Life Technologies, 11320033), Bovine Fetal Serum (BFS, Gibco), Trypsin 0.25% (Gibco by Lite Technologies), Antibiotic Penicilin Streptomycin (PENSTREP, Gibco by Life Technologies), LIVE / DEAD ™ Viability / Cytotoxicity Kit (Molecular Probes, 13224),

Reduced Graphene Oxide (rGO) was donated by CTNANO, UFMG, Brazil.

2.2 Preparation Pre-GelMA

The synthesis of gelatin methacryloyl was performed by solubilizing 10 g of gelatin in 100 ml of PBS (pH 7.4) at 50°C. Then, 4 g of MAA or 7 g of MAA were added to the gelatin solution to produce two different levels of methacrylation: low (LL) and high (HL), respectively. The solutions were stirred for 2 hours at 50°C, and dialyzed for 5 days against DI water, under agitation. The ungelled so-called pre-GeIMA was frozen and then lyophilized.

2.3 Preparation GelMA

To produce GelMA, a solution of 10 mg of 2-hydroxy-4'-(2-hydroxyethoxy) -2-methylpropiophenone (photoinitiator) in 1 ml of DI water and 100 mg of lyophilized pre-GelMA was submitted to UV light (wavelength in the range 360-480 nm, 6.9 mW / cm^2) for 10 minutes for light curing. The same amount of pre-GeIMA was used for the different levels of methacrylation to prepare GeIMA LL and GeIMA HL (low levels (LL) and high level (HL)).

2.4 Preparation GelMA NCC and GeMA rGO

The cellulose nanocrystals (NCC) were extracted from the bleached eucalyptus pulp, donated by the company Suzano Papel e Celulose. For CNC extraction, 30 mL of sulfuric acid (H_2SO_4, 65% by weight) was used for each 1 g of pulp. Acid hydrolysis was carried out at 40°C for 10 minutes under mechanical stirring at 300 rpm. The obtained suspension was diluted in water and ice cubes to stop the reaction, filtered, centrifuged at 4000 rpm for 20 minutes and transferred to cellulose membranes. Dialysis was performed in distilled water until it reached neutral pH.

To prepare GelMA NCC, 10 mg of the photoinitiator and 100 mg of lyophilized pre-GelMA were added in a 1 ml of DI water. Then, 5 or 10 wt. % of NCC in relation to pre-GelMA were incorporated into the solutions to produce GeIMA LL 5% NCC, GeIMA LL 10% NCC, GeIMA HL 5% NCC and GeIMA HL 10% NCC. Similarly, 20 wt. % of rGO was dispersed in the pre-GelMA solution to yield GeIMA LL rGO, and GeIMA HL rGO after photopolymerization.

After polymerization, hydrogels were washed with DI water and were freeze-dried for the characterization procedures.

2.5 Characterization and measurements of properties

2.5.1 Fourier transform Infrared spectroscopy (FTIR)

FTIR spectra were collected using the ATR Multi-Bounce apparatus in a Nicolet 6700 spectrophotometer. Spectra were collected after 64 scans with a resolution of 4 cm^{-1}.

2.5.2 Dynamic mechanical behavior

Dynamic mechanical analysis (DMA) was performed using a DMS 6100 SII Exstar equipment in compression. The hydrogels were cut into discs with 6.5 mm in height and 8 mm in diameter and were swollen in DI water prior to the test. The tests were performed with samples submerged in DI water at 37°C and frequencies ranging from 0.05Hz to 200Hz.

2.5.3 Cell culture

RKO AS45-1 tumor cell lines (Human Colon Carcinoma) acquired from the American Type Culture Collection (ATCC # CRL-2579) were cultured in DMEM High Glucose medium in 10% Bovine Fetal Serum (SFB) and in 1% streptomycin penicillin (PEN STREP). Cell lines were incubated in humidified enriched atmosphere containing 5% CO_2 at 37°C.

2.6 RKO encapsulation in hydrogels

To encapsulate cells in GelMA hydrogels, three solutions were prepared:

1- Solution FI: 1 ml of sterile Mili-Q water was heated in a 2 mL Eppendorf at 60°C with 10 mg of the photoinitiator;

2- Pre-GeIMA stock solution: 1 mL of DMEM High Glucose, 10 wt. % BFS and 1 wt. % PENSTREP were heated in a 2 ml Eppendorf at 60°C and 100 mg of lyophilized pre-GeIMA was added. The solution was mixed in Vortex and kept at 37°C;

3- Cell suspension: cells were counted in a Neubauer chamber and a cell suspension of 6.5 10^5 cells/mL was prepared.

The solutions were then combined for polymerization and cell encapsulation as described below:

500 µl of the pre-GeIMA stock solution, 50 µl of the FI solution and 450 µl of the cell suspension were combined to produce 1 mL of the cell dispersion in pre-GelMA aqueous solution. 450µl of this resulting solution was then used in each well of a 12-well plate, with a concentration of 3 10^5 cells/ml.

The plate was exposed to the incidence of ultraviolet light consisting of three 9W UVC lamps for 8 minutes and left in an oven at 37°C for 24 hours.

RKO cells were encapsulated in each type of hydrogels and the resulting hydrogels with cells were named as GeIMA LL_RKO, GeIMA LL 5% NCC_RKO, GeIMA LL 10% NCC_RKO, GeIMA LLrGO_RKO, GeIMA HL_RKO, GeIMA HL 5% NCC_RKO, GeIMA HL 10% NCC_RKO and GeIMA HL rGO_RKO.

All the labware used for the polymerization of the hydrogels was exposed to UV light from the flow hood for 20 minutes for sterilization purposes.

2.7 Cytotoxicity assays

2.7.1 Analysis of cell viability by MTT

To evaluate the cytotoxicity of the hydrogels, the MTT colorimetric assay was used.

Hydrogels without encapsulated cells were cut to approximately 4x4mm, sterilized for 1 hour in 70% alcohol, and after that time, they were washed 3x in MILI-Q water. For each wash, the hydrogels were submerged for 20 minutes in MILI-Q water.

The hydrogels were placed in direct contact with the cell strain (RKO AS45-1) for 24 hours and 48 hours. As a negative control (life control): cells were cultured in DMEM High Glucose, 10 wt. % BFS and 1 wt %. PENSTREP; as a positive control (death control): Hydrogen peroxide (H_2O_2) was added to the cell culture. Biological and experimental triplicates were performed. The reading was performed on a SpectraMax M5E microplate reader (Molecular Devices) at 550 nm.

2.7.2 Viability by LIVE/DEAD

For the live dead tests over 24 and 48 hours, hydrogels with embedded RKO cells were polymerized in 12-well plates, in triplicates. 300µl of the live / dead solution (2.0 µM EthD-1 (Ethidium Homodimer-1) and 1.0µM Calcein AM diluted in PBS) was added and the plate was viewed under an inverted fluorescence microscope (Calcein AM filter 09; EthD-1 filter 15).

The cell viability (%) was used to count cell viability: viable cells / total cell (viable and non-viable cells) x100.

2.8 Characterization of cells

2.8.1 Scanning electron microscopy (SEM)

Hydrogels containing embedded RKO were fixed with 2.5% glutaraldehyde for 1 hour. Then, the samples were washed twice with ice cold PBS (6 ± 2) °C. Then, they were dried by immersion in solutions of increasing concentration of ethanol/water (20%, 50%, 90%, 100% v / v) and finally vacuum dried in a desiccator for 24 hours. The samples were covered with gold.

2.8.2 Histological section

After 24 hours and 48 hours in an oven at 37 °C, GelMA LL_RKO and GelMA HL_RKO hydrogels were fixed with 4% formaldehyde and subsequently dehydrated, mounted, submitted to microtomy, stained with hematoxylin-eosin and assembled on glass slides.

3. Results and Discussion

3.1 Fourier-Transform Infrared Spectroscopy (FTIR)

In FTIR spectra of Figure 1A, the presence of gelatin in the hydrogels was verified by the existence of the absorption bands at 3316 cm^{-1} and 3079 cm^{-1} related to the NH group[9]. It is also possible to observe, at 1631 cm^{-1}, typical band of the C = O bond, characteristic of amide I, and absorbance bands at 1542 cm^{-1} and 1237 cm^{-1} related to amides II and III, respectively. The band related to the CH group was also observed at 1447 cm^{-1}.

Absorption bands associated with methacrylic anhydride can be seen in the spectra of hydrogels (Figure 1A) at 1034 cm^{-1} due to C-O bonds[10]. The methacrylic anhydride reacts with the primary amine groups in gelatin to lead to the addition of methacryloyl groups in the gelatin macromers[11]. GelMA crosslinking occurs when GelMA, in the presence of a photoinitiator, is exposed to UV light radiation. The absorption of UV light leads to the production of free radicals, and GelMA is then polymerized through C=C chain polymerization[12].

Absorption bands around 1100 cm^{-1} associated with C-O bonds in NCC can be observed in the spectra of LL 5% NCC, LL 10% NCC, HL 5% NCC and HL10% NCC in Figure 1B[13,14] and can be used to prove the presence of this nanocomponent in the hydrogels. In relation to the reduced graphene oxide presence in hydrogels, it is possible to note in the spectrum of the LL rGO sample an intense and wide band that goes from approximately 3700 to 2290 cm^{-1} referring to the OH axial deformation of carboxylic acids. An absorption band at 1700 cm^{-1} due to -C=O, commonly found in carboxylic acids, can also be associated with ketone carbonyl and aldehydes[15]. Absorption bands at 1228 cm^{-1}, attributed to C-OH stretch and at 1058 cm^{-1} referring to epoxides (-C-OC-) can also be identified in the spectrum of the hydrogel with rGO[16]. These absorption bands indicate that the produced rGO has several oxygen-containing groups such as epoxides, hydroxyls, carbonyls and carboxyls, related to the reaction with hydrazine hydrate[16].

3.2 Mechanical properties

Since tissues and organs in the body are most of the time subjected to dynamic mechanical loadings in a wet

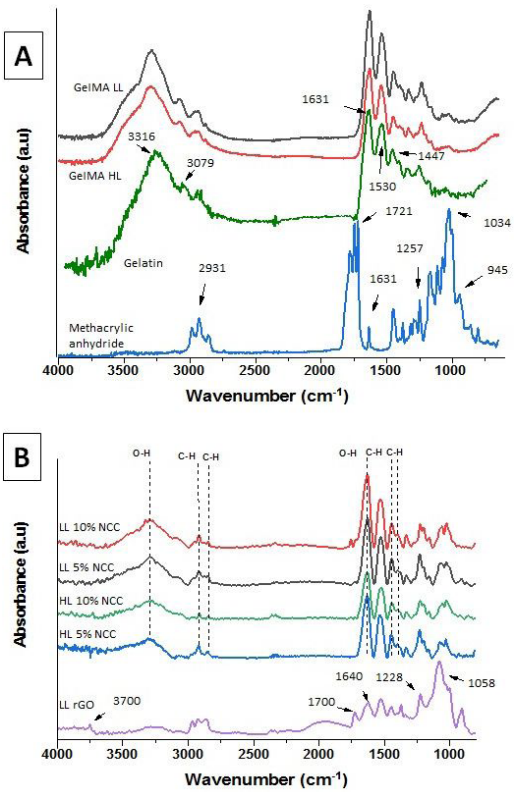

Figure 1. FTIR spectra of GelMA LL, GelMA HL, gelatin and methacrylic Anidride (A), and FTIR spectra of GelMA LL and GelMA HL containing cellulose nanocrystals and rGO (B).

environment (such as from the circulation of body fluids, shear forces between moving parts of the body, etc.), it is relevant to study the behavior of biomaterials in these conditions. Moreover, it also known that dynamic loads have a great impact on the performance of tissues and organs, by promoting cell migration, differentiation, growth and biomolecule expression[17,18]. In some applications involving organoids, the ability to tune the stiffness of the hydrogels to better match the properties of the pursued tissue (to reach, for example, high values of modulus, such as 30 kPa) is desirable[19]. Elastic modulus of normal soft tissues was shown to range between 0.5 kPa (brain), 10 kPa (dermis) and 12 kPa (muscle), while the modulus of diseased fibrotic tissues is higher (15–100 kPa)[20]. For example, normal breast tissue shows moduli between 6-10 kPa. This same tissue with intermediate grade of mammary tumor has an elastic modulus in the 15-20 kPa range, while an advanced grade of tumor can reach 40 kPa[20].

Several approaches have been proposed and tested to improve the mechanical properties of hydrogels, such as the preparation of hybrid hydrogels and hydrogels with double networks[19]. However, most of the mechanical properties reported for the prepared hydrogels were measured in static conditions, such as by using conventional stress-strain tests.

Thus, GelMA hydrogels were tested in a dynamic mechanical (DMA) environment (Figure 2A), in which mechanical loads were applied in frequencies ranging from 0.05 to 200 Hz while immersed in water at 37 °C.

In Figure 2B, only dynamic mechanical data regarding GelMA LL hydrogels are revealed to check the effect of the incorporation of nanocomponents (either NCC or rGO) on the dynamic mechanical behavior of the hydrogels. Results show that the presence of NCC in the hydrogels led to higher values of elastic storage modulus (E´) when compared to pure GelMA LL hydrogels, demonstrating the powerful capacity of NCC to increase the stiffness of GelMA hydrogels. Moreover, a traditional behavior of E´ for viscoelastic materials was observed in frequencies ranging from 0.05 to 20Hz for all the tested hydrogels: a gradual increase of the storage modulus with frequency, meaning that shorter times of load application can favor less ability of the polymer chains to respond to the mechanical stimulus. For higher frequencies (≥ 100 Hz), both GelMA LL hydrogels and GelMA LL rGO seemed to collapse with an abrupt decay in the E´ measurements. Otherwise, GelMA LL hydrogels with 10% NCC were able to withstand higher frequencies, demonstrating the ability of NCC to mechanically reinforce and stabilize the hydrogels. Results in Figure 2B also show that it is possible to tune the stiffness of the GelMA LL hydrogels from kPa to MPa by the incorporation of NCC.

Lower values of E´ of GelMA rGO in respect to pure GelMA were noted in Figure 2B. This is due to the fact that hydrogels with rGO were observed to have a lower degree of crosslinking than other GelMA hydrogels due to the reduced penetration of UV light during polymerization in the samples with rGO. The low degrees of crosslink for the GelMA LL rGO could also be detected by measuring the swelling degree (SD) of the hydrogel after 24 hours in DI water. $SD(\%) = \frac{M_f - M_0}{M_0} \times 100$, where M_f and M_0 are the weight of the sample after and before swelling, respectively. The value of SD was approximately 500% for GelMA LL and 1600% for the GelMA LL rGO. Therefore, the swelling capacity of the hydrogels with rGO was more than three times the swelling ability of pure hydrogels (with no rGO), indicating again a lower degree of crosslink. The fact that GelMA LL rGO has a lower degree of crosslinking (due to low levels of photopolymerization conversion) is the reason why this hydrogel displayed low values of elastic modulus (even lower than GelMA LL) and low stability at higher frequencies.

3.3 Cell viability

The results of cell viability by MTT are presented in Figure 3. These MTT tests were performed in hydrogels with no encapsulated cell to study the eventual toxicity of GelMA hydrogels and hydrogels containing nanocomponents. Thus, hydrogels were put in contact with RKO cell for 24 and 48 hours to check cell viability by the MTT protocol. Results in Figure 3 reveal that there was no statistical difference in

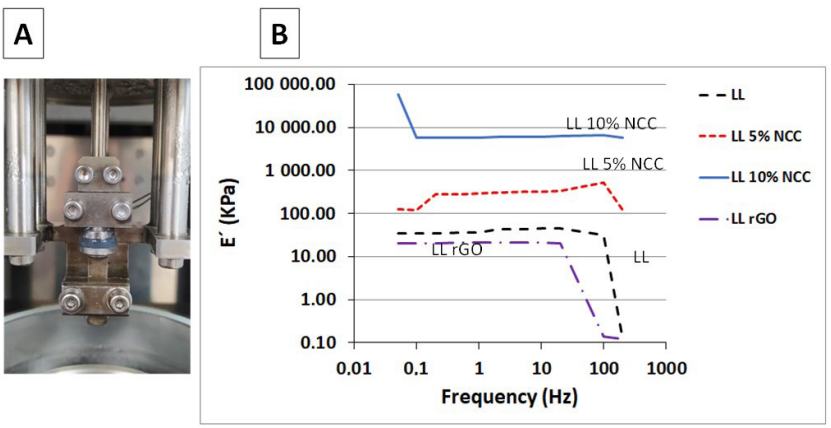

Figure 2. (A) Photo of a swollen hydrogel between compression plates just prior of being dipped in DI water bath to be tested under dynamic mechanical conditions (DMA); (B) Storage elastic modulus as a function of frequency for GelMA LL hydrogels with NCC or rGO.

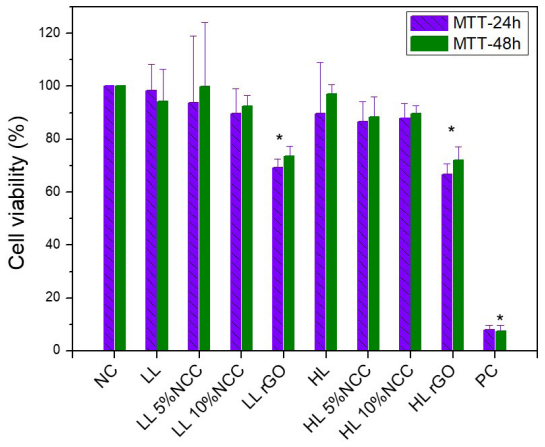

Figure 3. Cell viability results of RKO cells in contact with hydrogels with no encapsulated cells by MTT. Cell viability after (A) 24 hours and (B) after 48 hours. NC = negative control (life control); PC = positive control (death control). *indicates significant difference.

the viability of RKO cells, when this behavior is compared between 24 and 48 hours for each type of sample.

Viability values remained above 85%, for GeIMA LL and GeIMA HL, and in their derivatives containing 5% and 10% NCC (values above which the materials are considered non-cytotoxic). There was no significant difference in cell viability when compared to the negative control group (CV) of the MTT assay.

However, GeIMA LL rGO and HL rGO hydrogels (i.e. hydrogels with rGO) showed lower viability values (approximately 70%) that were significantly different from the negative control. These lower values of cell viability may be associated with the lower levels of stability of these hydrogels due to their lower degrees of crosslink. It was observed that the photopolymerization of pre-GelMA with rGO was less effective, leading to hydrogels with lower levels of crosslink and higher abilities to swell in water. Thus, it can be proposed that eventual unreacted specie can leach out of the Gel rGO hydrogels during the *in vitro* tests to lead to higher levels of cell toxicity.

Cell viability measured by LIVE DEAD assays is presented in Figure 4. In this case, GelMA hydrogels with encapsulated RKO cells were tested to check the possibility of keeping cells alive while encapsulated within the hydrogels. Figure 4A shows the number of cells found in all hydrogels and in the RKO control group measured by Image J from the images recorded by the fluorescence microscope. The number of cells counted in hydrogels at 48 hours in an oven at 37 °C was significantly greater than the hydrogels at 24 hours. An increase in cell density after 48 hours of culturing, when compared to 24 hours of culturing, indicates that embedded cells were able to proliferate within the hydrogels due to a highly porous and chemically adequate environment that resembles the extracellular matrix provided by GeIMA[16].

The number of cells in the control group (RKO) was much higher than the cells counted in the hydrogels, but it is worth mentioning that the RKO cells were cultured in 2D culture, with the reading being linear, while the cells

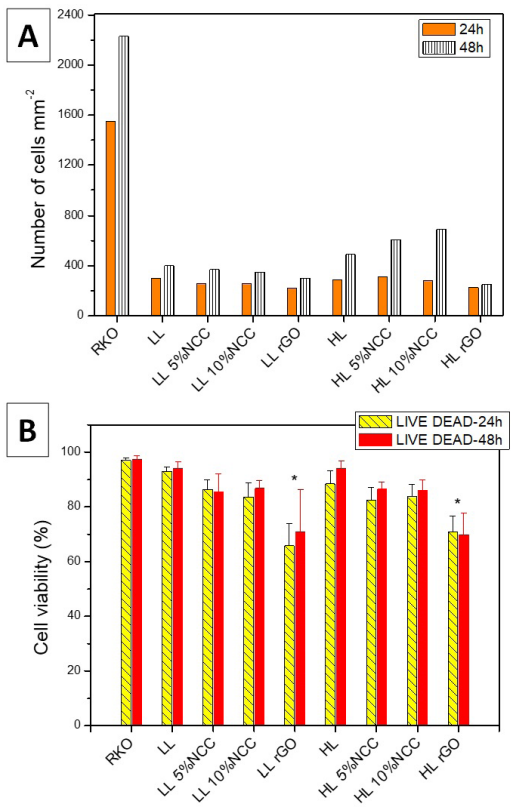

Figure 4. (A) Number of RKO cells encapsulated in the hydrogels after 24 and 48 hours of culture; (B) cell viability results by LIVE DEAD of hydrogels containing RKO in the period of 24 hours and 48 hours. *indicates significant difference.

were counted in the hydrogels in only one plane of their three-dimensional structure. For hydrogels with higher levels of methacryloyl substitution (GelMA HL), results in Figure 4A showed that the incorporation of NCC tended to lead to higher number of cell per area after 48 hours when compared to pure GelMA HL hydrogels. This result may be related to a more favorable ambient for cell growth, as possibly due to a higher network stability (Figure 2B) combined with higher values of stiffness (Figure 2B) for hydrogels with NCC, since tumor cells seem to be more well accommodate in stiffer extracellular matrices[20].

LIVE DEAD cell viability results (Figure 4B) agree with cell viability results reported by MTT assays (Figure 3), by showing that cell viability values above 85% were observed for all hydrogels with encapsulated RKO cells (with no statistical difference regarding the RKO control), except for hydrogels with rGO that had lower viability values (around 70%). This result also proves that the polymerization procedure did not affect the viability of the encapsulated cells.

Figures 5 and 6 show optical microscopy (OM) and electron microscopy (SEM) images from LIVE DEAD tests. The reported images indicated the presence of viable cells in GelMA hydrogels. It was possible to observe an increase in cell density after 48 hours of culturing, when compared to 24 hours.

The images in Figure 5 of the histological section (HE) of the GeIMA LL RKO and HL RKO hydrogels also

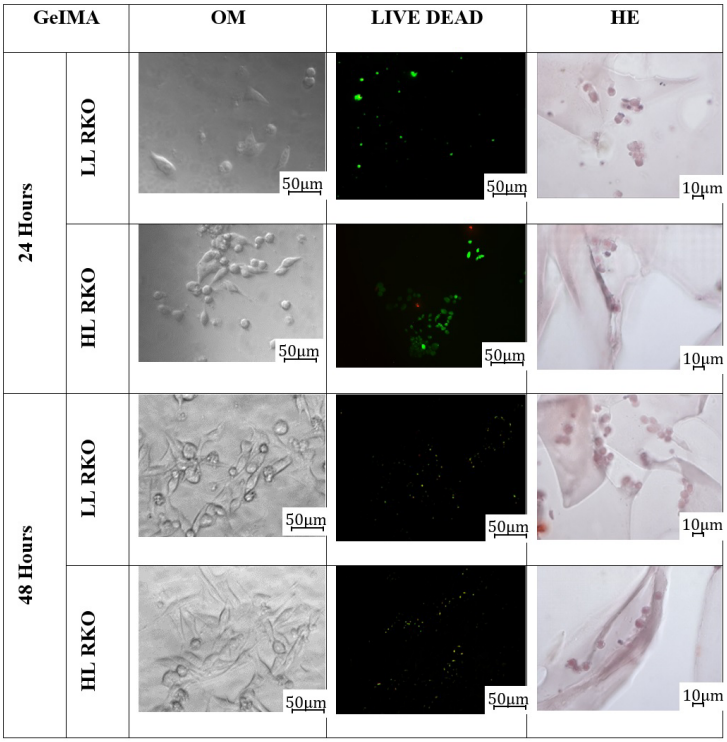

Figure 5. Images of the encapsulated RKO cell in the GelMA LL and GelMA HL RKO hydrogels at 24 and 48 hours, obtained by optical microscopy (OM), stained by the LIVE DEAD assay and by hematoxylin eosin (HE) staining.

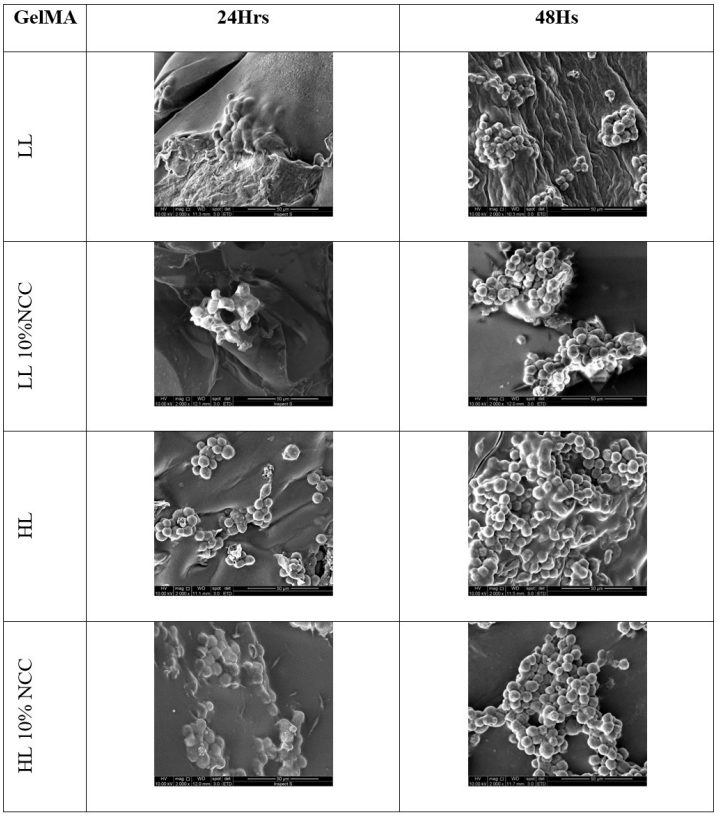

Figure 6. SEM images (2000X) of embedded RKO cells in the cross sections of the hydrogels.

demonstrate that the embedded cells with elliptical and central nuclei were able to proliferate. Elongated cells can also be seen in images of Figure 5.

SEM images of the cross-section of hydrogels (Figure 6) also reveal the ability of the embedded cells to proliferate. Moreover, cells were also able to start to form organized larger groups after 48h that can yield full integrated tumor tissues as the main idea of manufacturing tumor organoids.

4. Conclusion

Tumor organoids can provide tools for studying the proliferation of cancer cells as well as the efficacy of different anti-cancer treatments. Hydrogels emerge as a potential host for cancer cells to form tumor organoids since they have high porosity and high levels of hydration that can be tuned to yield similarities to natural extracellular matrices. Gelatin-based photopolymerizable hydrogels (GelMA) can be considered a promising hydrogel for this type of application, since they possess bioactive sequences of amino acids as well as high processability and capacity for encapsulating cells. In this work, we have explored to possibility of modifying the structure of GelMA to verify its effect on properties and cancer cell encapsulation and proliferation. To this end, the degree of methacryloyl substitution in gelatin (closely related to the crosslink density) and the incorporation of nanocomponents in the hydrogels, such as cellulose nanocrystals (NCC) and reduced graphene oxide (rGO) were tested. Since natural tissues are submitted to dynamic forces during their lifetimes, hydrogels were submitted experimentally to similar conditions, in which they were submerged in water at 37°C and subjected to cyclic compression loads that varied from 0.05 to 200 Hz. Results demonstrated that hydrogels with NCC were able to withstand high frequencies (up to 200 Hz), while hydrogels with no NCC mechanically failed at lower frequencies. Moreover, GelMA with rGO were not fully crosslinked due to restriction of photopolymerization conversion. This fact led to hydrogels with lower storage modulus and lower levels of mechanically stability. Viability tests demonstrated that RKO cells were able to be encapsulated within hydrogels. These cells were also able to proliferate within the hydrogel. Hydrogels with high levels of methacryloyl substitution and containing NCC show higher proliferation rates as a possible consequence of higher levels of network stability and stiffness that may reflect more common tumor environment. SEM images of the cross-section of the hydrogels showed that RKO embedded cells can form large colonies of cells in 48 hours of culturing that indicated the possibility of using gelatin derived hydrogels as a matrix to support the proliferation of cancer cells and formation of tumor organoids.

5. Author's Contribution

- **Conceptualization –** Sarah Oliveira Lamas de Souza; Luciana Maria Silva; Rodrigo Lambert Oréfice.
- **Data curation –** Sarah Oliveira Lamas de Souza; Sérgio Mendes de Oliveira; Catarina Paschoalini Lehman; Mercês Coelho da Silva.
- **Formal analysis –** Sarah Oliveira Lamas de Souza; Luciana Maria Silva; Rodrigo Lambert Oréfice.
- **Funding acquisition –** Rodrigo Lambert Oréfice.
- **Investigation –** Sarah Oliveira Lamas de Souza; Sérgio Mendes de Oliveira; Catarina Paschoalini Lehman; Mercês Coelho da Silva; Luciana Maria Silva; Rodrigo Lambert Oréfice.
- **Methodology –** Sarah Oliveira Lamas de Souza; Sérgio Mendes de Oliveira; Catarina Paschoalini Lehman; Mercês Coelho da Silva.
- **Project administration –** Rodrigo Lambert Oréfice.
- **Resources –** Rodrigo Lambert Oréfice.
- **Software –** NA.
- **Supervision –** Rodrigo Lambert Oréfice.
- **Validation –** Luciana Maria Silva; Rodrigo Lambert Oréfice.
- **Visualization –** Luciana Maria Silva; Rodrigo Lambert Oréfice.
- **Writing – original draft –** Sarah Oliveira Lamas de Souza; Rodrigo Lambert Oréfice.
- **Writing – review & editing –** Sarah Oliveira Lamas de Souza; Rodrigo Lambert Oréfice.

6. Acknowledgements

The authors thank CAPES, CNPq and FAPEMIG for their financial support.

7. References

1. Aamodt, J. M., & Grainger, D. W. (2016). Extracellular matrix-based biomaterial scaffolds and the host response. *Biomaterials*, *86*, 68-82. http://dx.doi.org/10.1016/j.biomaterials.2016.02.003. PMid:26890039.
2. Nuciforo, S., Fofana, I., Matter, M. S., Blumer, T., Calabrese, D., Boldanova, T., Piscuoglio, S., Wieland, S., Ringnalda, F., Schwank, G., Terracciano, L. M., Ng, C. K. Y., & Heim, M. H. (2018). Organoid models of human liver cancers derived from tumor needle biopsies. *Cell Reports*, *24*(5), 1363-1376. http://dx.doi.org/10.1016/j.celrep.2018.07.001. PMid:30067989.
3. Lancaster, M. A., & Knoblich, J. A. (2014). Generation of cerebral organoids from human pluripotent stem cells. *Nature Protocols*, *9*(10), 2329-2340. http://dx.doi.org/10.1038/nprot.2014.158. PMid:25188634.
4. Maenhoudt, N., Defraye, C., Boretto, M., Jan, Z., Heremans, R., Boeckx, B., Hermans, F., Arijs, I., Cox, B., Van Nieuwenhuysen, E., Vergote, I., Van Rompuy, A.-S., Lambrechts, D., Timmerman, D., & Vankelecom, H. (2020). Developing organoids from ovarian cancer as experimental and preclinical models. *Stem Cell Reports*, *14*(4), 717-729. http://dx.doi.org/10.1016/j.stemcr.2020.03.004. PMid:32243841.
5. Thakuri, P. S., Liu, C., Luker, G. D., & Tavana, H. (2018). Biomaterials-based approaches to tumor spheroid and organoid modeling. *Advanced Healthcare Materials*, *7*(6), e1700980. http://dx.doi.org/10.1002/adhm.201700980. PMid:29205942.
6. Lima, F., Melo, W. G., Braga, M. F., Vieira, E., Câmara, J. V., Pierote, J. J., Argôlo, N., No., Silva, E., Fo., & Fialho, A. C. (2021). Chitosan-based hydrogel for treatment of temporomandibular joint arthritis. *Polímeros: Ciência e Tecnologia*, *31*(2), e2021019. http://dx.doi.org/10.1590/0104-1428.20210026.

7. Huang, J., Jiang, Y., Ren, Y., Liu, Y., Wu, X., Li, Z., & Ren, J. (2020). Biomaterials and biosensors in intestinal organoid culture, a progress review. *Journal of Biomedical Materials Research. Part A*, *108*(7), 1501-1508. http://dx.doi.org/10.1002/jbm.a.36921. PMid:32170907.
8. Dong, Z., Yuan, Q., Huang, K., Xu, W., Liu, G., & Gu, Z. (2019). Gelatin methacryloyl (Gelma)-based biomaterials for bone regeneration. *RSC Advances*, *9*(31), 17737-17744. http://dx.doi.org/10.1039/C9RA02695A. PMid:35520570.
9. Soares, G. O. N., Lima, F. A., Goulart, G. A. C., & Oréfice, R. L. (2021). Physicochemical characterization of the gelatin/polycaprolactone nanofibers loaded with diclofenac potassium for topical use aiming potential anti-inflammatory action. *International Journal of Polymeric Materials*, *71*(17), 1303-1318. http://dx.doi.org/10.1080/00914037.2021.1962875.
10. Sun, M., Sun, X., Wang, Z., Guo, S., Yu, G., & Yang, H. (2018). Synthesis and properties of gelatin methacryloyl (Gelma) hydrogels and their recent applications in load-bearing tissue. *Polymers*, *10*(11), 1290. http://dx.doi.org/10.3390/polym10111290. PMid:30961215.
11. Zhu, M., Wang, Y., Ferracci, G., Zheng, J., Cho, N.-J., & Lee, B. H. (2019). Gelatin methacryloyl and its hydrogels with an exceptional degree of controllability and batch-to-batch consistency. *Scientific Reports*, *9*(1), 6863. http://dx.doi.org/10.1038/s41598-019-42186-x. PMid:31053756.
12. Krishnamoorthy, S., Noorani, B., & Xu, C. (2019). Effects of encapsulated cells on the physical–mechanical properties and microstructure of gelatin methacrylate hydrogels. *International Journal of Molecular Sciences*, *20*(20), 5061. http://dx.doi.org/10.3390/ijms20205061. PMid:31614713.
13. Kong, J., & Yu, S. (2007). Fourier transform infrared spectroscopic analysis of protein secondary structures. *Acta Biochimica et Biophysica Sinica*, *39*(8), 549-559. http://dx.doi.org/10.1111/j.1745-7270.2007.00320.x. PMid:17687489.
14. Mertz, G., Fouquet, T., Becker, C., Ziarelli, F., & Ruch, D. (2014). A methacrylic anhydride difunctional precursor to produce a hydrolysis-sensitive coating by aerosol-assisted atmospheric plasma process: hydrolysis-sensitive coating deposited by aerosol assisted atmospheric plasma. *Plasma Processes and Polymers*, *11*(8), 728-733. http://dx.doi.org/10.1002/ppap.201400050.
15. Edmondson, R., Broglie, J. J., Adcock, A. F., & Yang, L. (2014). Three-dimensional cell culture systems and their applications in drug discovery and cell-based biosensors. *Assay and Drug Development Technologies*, *12*(4), 207-218. http://dx.doi.org/10.1089/adt.2014.573. PMid:24831787.
16. Grenier, J., Duval, H., Barou, F., Lv, P., David, B., & Letourneur, D. (2019). Mechanisms of pore formation in hydrogel scaffolds textured by freeze-drying. *Acta Biomaterialia*, *94*, 195-203. http://dx.doi.org/10.1016/j.actbio.2019.05.070. PMid:31154055.
17. Nichol, J. W., Koshy, S. T., Bae, H., Hwang, C. M., Yamanlar, S., & Khademhosseini, A. (2010). Cell-laden microengineered gelatin methacrylate hydrogels. *Biomaterials*, *31*(21), 5536-5544. http://dx.doi.org/10.1016/j.biomaterials.2010.03.064. PMid:20417964.
18. Achterberg, V. F., Buscemi, L., Diekmann, H., Smith-Clerc, J., Schwengler, H., Meister, J.-J., Wenck, H., Gallinat, S., & Hinz, B. (2014). The nano-scale mechanical properties of the extracellular matrix regulate dermal fibroblast function. *The Journal of Investigative Dermatology*, *134*(7), 1862-1872. http://dx.doi.org/10.1038/jid.2014.90. PMid:24670384.
19. Yue, K., Trujillo-de-Santiago, G., Alvarez, M. M., Tamayol, A., Annabi, N., & Khademhosseini, A. (2015). Synthesis, properties, and biomedical applications of gelatin methacryloyl (Gelma) hydrogels. *Biomaterials*, *73*, 254-271. http://dx.doi.org/10.1016/j.biomaterials.2015.08.045. PMid:26414409.
20. Magno, V., Meinhardt, A., & Werner, C. (2020). Polymer hydrogels to guide organotypic and organoid cultures. *Advanced Functional Materials*, *30*(48), 2000097. http://dx.doi.org/10.1002/adfm.202000097.

Received: Mar. 22, 2022
Revised: Feb. 14, 2023
Accepted: May 05, 2023